Crystal structures of the *Arabidopsis thaliana* proliferating cell nuclear antigen 1 and 2 proteins complexed with the human p21 C-terminal segment

Wojciech Strzalka,[1†] Takuji Oyama,[2†] Kazuo Tori,[2] and Kosuke Morikawa[2]*

[1]Department of Molecular Genetics, Faculty of Biochemistry, Biophysics and Biotechnology, Jagiellonian University, 30-387 Krakow, Poland

[2]The Takara Bio Endowed Division, Open Laboratories of Advanced Bioscience and Biotechnology (OLABB), Institute for Protein Research, Osaka University, Suita, Osaka 565-0874, Japan

Abstract: The proliferating cell nuclear antigen (PCNA) is well recognized as one of the essential cellular components of the DNA replication machinery in all eukaryotic organisms. Despite their prominent importance, very little biochemical and structural information about plant PCNAs is available, in comparison with that obtained from other eukaryotic organisms. We have determined the atomic resolution crystal structures of the two distinct *Arabidopsis thaliana* PCNAs (*At*PCNA), both complexed with the C-terminal segment of human p21. Both *At*PCNAs form homotrimeric ring structures, which are essentially identical to each other, including the major contacts with the p21 peptide. The structure of the amino-terminal half of the p21 peptide, containing the typical PIP box sequence, is remarkably similar to those observed in the previously reported crystal structures of the human and archaeal PCNA-PIP box complexes. Meanwhile, the carboxy-terminal halves of the p21 peptide in the plant PCNA complexes are bound to the protein in a unique manner, most probably because of crystal packing effects. A surface plasmon resonance analysis revealed high affinity between each *At*PCNA and the C-terminal fragment of human p21. This result strongly suggests that the interaction is functionally significant, although no plant homologs of p21 have been identified yet. We also discovered that *At*PCNA1 and *At*PCNA2 form heterotrimers, implying that hetero-PCNA rings may play critical roles in cellular signal transduction, particularly in DNA repair.

Keywords: *Arabidopsis thaliana*; PCNA; crystal structure; X-ray diffraction

Introduction

Proliferating cell nuclear antigen (PCNA) is one of the most important proteins in eukaryotic cells. It was dis-

covered as an autoantigen of patients suffering from the immunological disorder, systemic lupus erythematosus.[1] The first function described for PCNA was its role as a DNA polymerase δ accessory protein required for new DNA strand synthesis.[2–4] The crystal structures of the yeast and human PCNAs provided important insights into the functional roles of PCNA in the replication process.[5,6] Moreover, crystallographic studies of functional PCNA homologs from *Pyrococcus furiosus*,[7] *E. coli*,[8] and bacteriophage RB69[9] revealed that these homologs form essentially the same architecture as the eukaryotic PCNA. The eukaryotic and

archaeal PCNAs, as well as the RB69 bacteriophage gp43 protein, in common form homotrimeric ring-shaped architectures accommodating a DNA duplex, similar to the *E. coli* DNA polymerase III β subunit (β-clamp), where only two subunits encircle the DNA as a homodimer. It is generally considered that PCNA, with the pseudo-sixfold symmetry, can slide along double-stranded DNA.[5–9] Thus, PCNA is generally called the sliding clamp, which can serve as a docking platform for many proteins involved in DNA metabolism. Further studies on PCNA demonstrated that it plays a crucial role not only in DNA replication but also in DNA repair, cell cycle regulation, and apoptosis.[10] Detailed analyses of the yeast and animal PCNAs led to the identification and characterization of more than 50 PCNA-interacting proteins.[11] Although the living organisms in the animal, plant, fungal, and archaeal kingdoms evolved from each other in ancient times, the most basic mechanism responsible for DNA replication seems to be highly conserved among them. The best example supporting this notion was the identification of *PCNA* genes in different species, such as yeast: budding yeast[12] and fission yeast[13]; animals: human,[14] rat,[15] mouse,[16] and *Drosophila*[17]; plants: carrot,[18] maize,[19,20] rice,[21] and common bean[22]; as well as archaeon: *Pyrococcus furiosus*.[23]

Furthermore, experimental results obtained using the yeast and *Drosophila* PCNAs revealed that these two molecules can functionally substitute for mammalian PCNA in DNA replication assays.[24,25] It was also demonstrated that recombinant rice PCNA stimulates the enzymatic activity of DNA polymerase δ from human cells.[26] Other studies on mammalian PCNAs showed that they stimulate the activity and processivity of two wheat δ-like polymerases.[27] Another important result, highlighting the highly conserved function of PCNA, described the stable complex formation between purified pea PCNA and human cyclin-dependent kinase inhibitor, p21/WAF-1.[28] This suggests that the p21 protein, induced by the DNA damage-induced cell-cycle growth arrest, targets at least two proteins, the G1-cyclin-dependent kinases (CDK) and PCNA. It was also shown that the p21 protein contacts the plant PCNA via its C-terminal segment. Thus, the atomic structure of the plant PCNA in complex with human p21 could provide useful insights into putative conservation of p21 homologs in plants.

In this study, we successfully purified and crystallized the recombinant *At*PCNA1 and 2 proteins, both complexed with the C-terminal fragment of human p21, and solved the three-dimensional (3D) structures of both complexes. These structures demonstrated that *At*PCNA1 and 2 indeed adopt identical architectures, which are typical of the sliding clamp with the pseudo-sixfold symmetry. These structures also provided important insights into the possible presence of a potential p21 homolog in plant cells.

Results and Discussion

### General architectures of *At*PCNA1 and 2

The plant *At*PCNA1 and *At*PCNA2 molecules, both complexed with the p21 peptide, were crystallized under similar crystallization conditions. We obtained two crystal forms (form 1 and form 2), with different space groups and unit cell constants (Supporting Information Table I and Fig. 1), although the molecular arrangements within the crystal lattice were similar to each other. We determined the *At*PCNA1-p21 complex structure in form 1 at 2.0 Å resolution and the *At*PCNA2 complex structure in form 2 at 2.5 Å resolution. The PCNAs form homotrimeric ring structures in both crystal forms [Fig. 1(A)], and the overall structures of *At*PCNA1 and *At*PCNA2 are almost the same, including the major contacts with the p21 peptide. *At*PCNA1 and *At*PCNA2 share 96% amino acid identity in their sequences [Fig. 1(B)], with only eight different amino acid residues. These different amino acids are not involved in either the p21 peptide interaction or the subunit interfaces [Fig. 1(C)]. Indeed, the two PCNAs are well superimposed on each other, with an RMSD of 0.4 Å. Therefore, our description of the overall structure and the detailed views of the interactions with the bound peptide will primarily be based on the higher resolution structure of the *At*PCNA1-p21 complex.

The plant PCNA forms the homotrimeric architecture, which exhibits the domain configuration with a pseudo-sixfold symmetry. The single subunit is composed of two structural domains, each containing a long, interdomain connecting loop (ID-loop, Fig. 1). Overall, the plant PCNA structure is similar to those of the previously reported PCNAs from human, yeast, archaea, and bacteriophage, highlighting the remarkable structural conservation across the domains of life [Fig. 1(B)].[5–7,9]

Interactions of the p21 peptide with *At*PCNA1 and 2

Figure 2(A,B) shows a structural view of the interactions between the plant *At*PCNA1 and the p21 peptide. The amino-terminal half of the p21 peptide, containing the typical PIP box sequence,[29] is bound to the PIP box binding pocket of *At*PCNA1. The protein–peptide interaction is mainly hydrophobic, and this part of the p21 peptide forms a one-turn helix, with Met147, a key residue of PIP, located at the bottom of the binding pocket [Fig. 2(B)]. This interaction mode is strikingly similar to those observed in the previously reported crystal structures, including the human and archaeal PCNA-PIP box complexes.[6,30]

On the other hand, the carboxy-terminal half of the p21 peptide is bound to the plant PCNA in a unique and unexpected manner. In the human PCNA-p21 peptide complex,[6] the carboxy-terminal half of the peptide interacts with the ID-loop to form an antiparallel β structure. In contrast, in the plant *At*PCNA1-
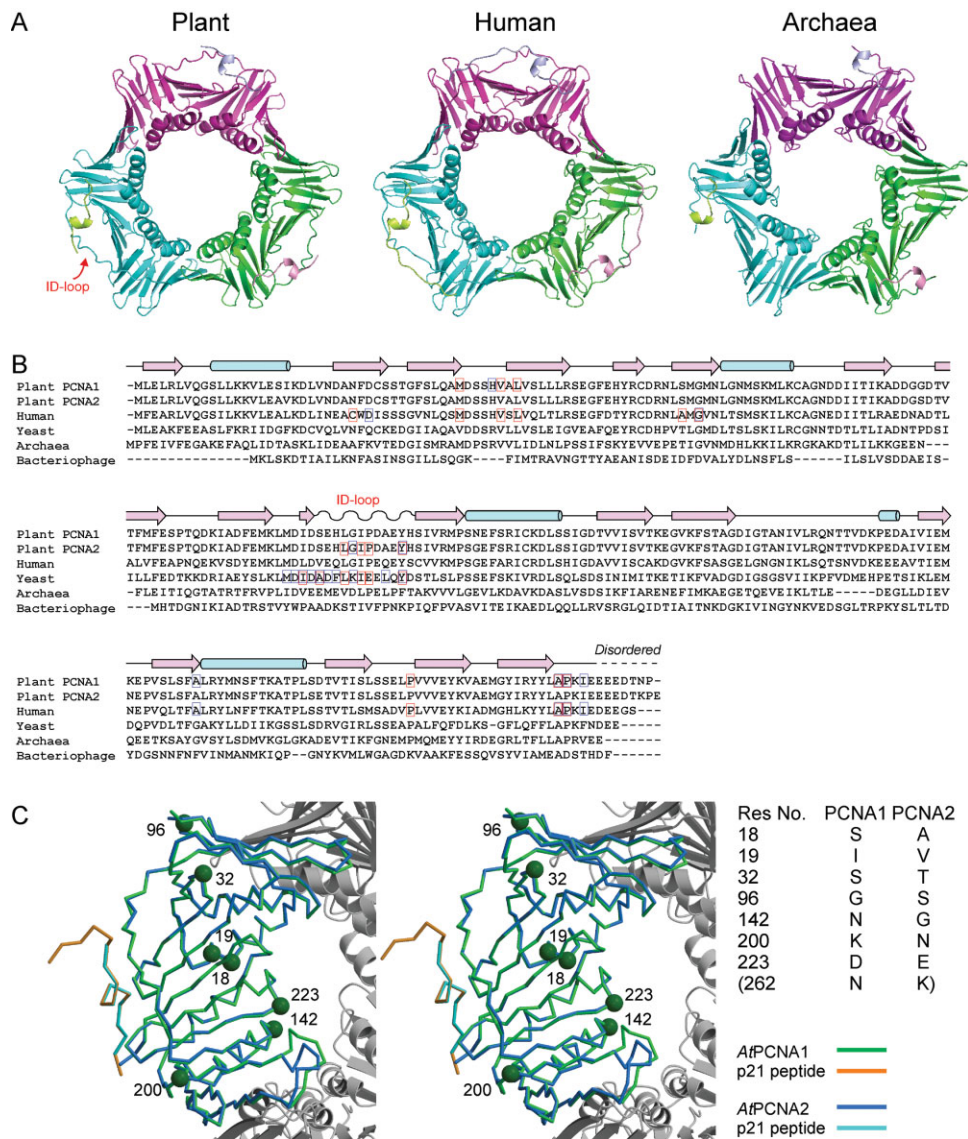
Figure 1. Crystal structure of the *Arabidopsis thaliana* PCNA (*At*PCNA)—p21 peptide complex. (**A**) Overall structure of *At*PCNA in comparison with those of the human and archaeal PCNAs. An interdomain connecting loop on *At*PCNA is depicted by an arrow. (**B**) Structure-based sequence alignment. Secondary structure elements are indicated by cylinders for α-helices and arrows for β-sheets. On the *At*PCNA1 and human PCNA sequences, the residues that interact with the p21-peptide are marked with red (hydrophobic) and blue (hydrophilic) boxes, respectively. (**C**) Comparison between *At*PCNA1 and *At*PCNA2. The superimposed structures are shown by a stereo pair. *At*PCNA1, the p21 peptide bound to *At*PCNA1, *At*PCNA2, and the peptide bound to *At*PCNA2, are colored green, orange, blue, and cyan, respectively. The two adjacent subunits forming a trimer ring of *At*PCNA1 are shown by gray ribbons. The different amino acids between *At*PCNA1 and *At*PCNA2 are highlighted. Asn262 of *At*PCNA1 and Lys262 of *At*PCNA2 were disordered in the structures.

p21 peptide complex crystal structure, the same part of the peptide does not contact the ID-loop. Instead, it protrudes out of the molecule and interacts with another p21 peptide bound to the neighboring PCNA subunit [Fig. 2(C) and Supporting Information Fig. 2].

These distinct binding modes between the human and plant proteins are probably derived from crystal packing effects. In fact, in the crystal lattice, the ID-loop of the plant PCNA extensively contacts the same segment in the adjacent subunit (Supporting Information Fig. 2). This contact mode, which was not observed in the human structure, appears to block the

normal interaction between the carboxy-terminal part of p21 and the plant PCNA. On the other hand, a conservation map, generated using the program ConSurf,[31] indicated that the p21 peptide binding surface comprises highly conserved amino acid residues [Fig. 2(D)]. Therefore, a similar binding mode to that in the human complex structure would exist in solution. In fact, our SPR analysis strongly supported this interpretation, as described in the following section.

Furthermore, a minor difference was discovered when the plant and human PCNA structures were compared. In the human structure, Ile158 of p21

Arabidopsis thaliana PCNA Crystal Structure
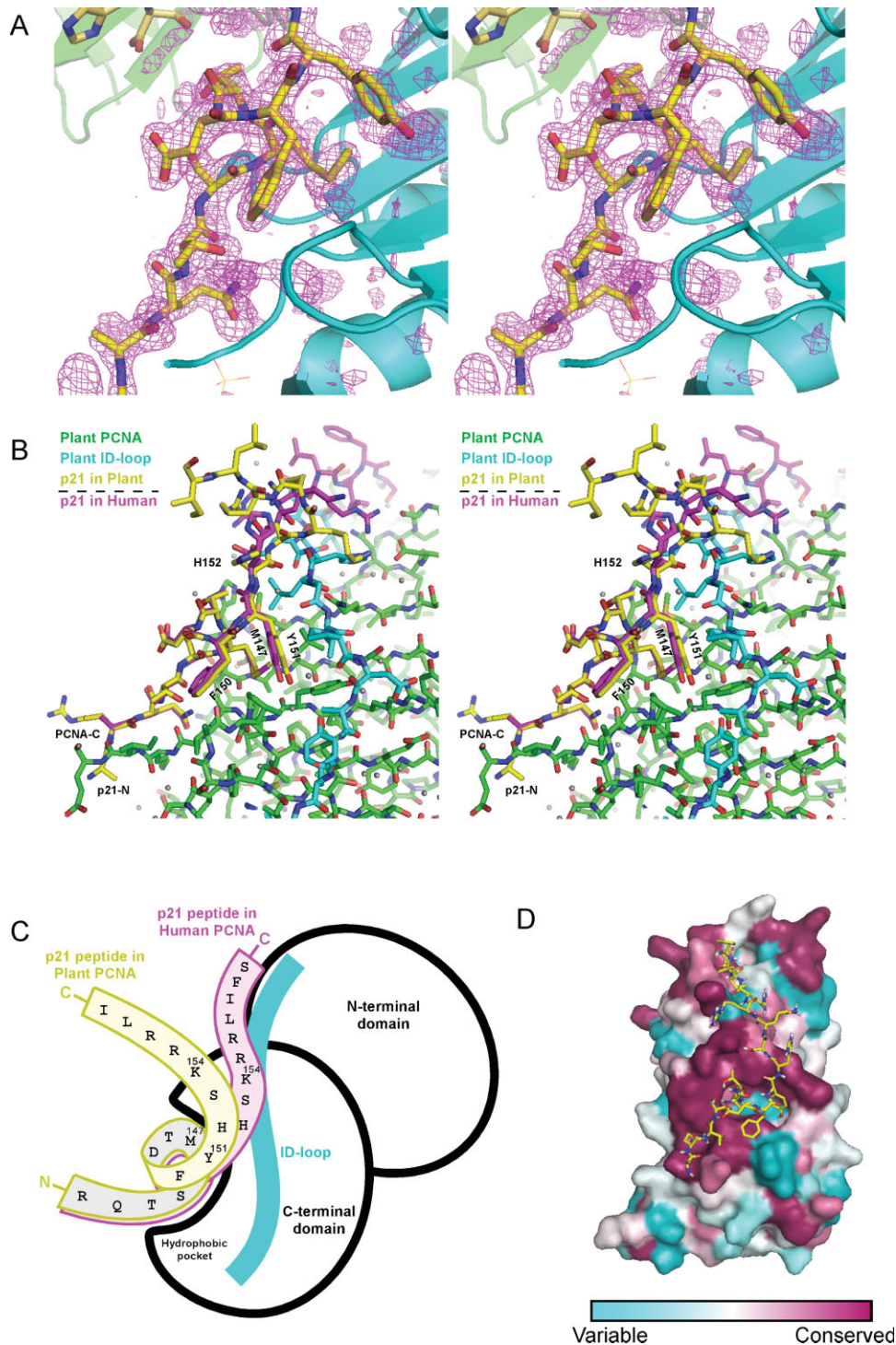
Figure 2. Interaction between *At*PCNA1 and the p21 peptide. (**A**) Stereo view of an omit F_o-F_c map for the bound p21 peptide. The map was calculated using the final model and contoured at 2.5σ. (**B**) Closeup view of the p21 peptide binding site. The ID-loop carbon atoms are colored cyan, and the p21 peptide carbons are yellow. The p21 peptide bound to human PCNA is superimposed on the plant PCNA structure, and is shown with magenta-colored carbon atoms. *At*PCNA lacks interactions with the C-terminal half of the p21 peptide, in a binding area formed by three segments, 27–29, 67–69, 119–125, when compared with human PCNA, because of the different conformation of the bound peptide. (**C**) Schematic view of the *At*PCNA-p21 peptide interaction, in comparison with that of human PCNA. (**D**) Conservation map generated using "Conserf." The peptide was taken from the human PCNA complex.

points toward the surface of PCNA and contacts the side-chain atoms of Cys27 and Ala67, which are replaced by Asn27 and Ser67, respectively, with larger side chains in the plant PCNA (Supporting Information Fig. 2). These substitutions may be another factor underlying the distinct binding mode.

Binding of the p21 peptide to AtPCNAs

To analyze the strength of the interactions between the short fragment of the p21 peptide, used for the crystallographic analyses, and the *Arabidopsis* PCNA1 and PCNA2 proteins in solution, we performed surface plasmon resonance (SPR) analysis. In fact, such an interaction between a plant PCNA and a short fragment of human p21 was previously reported.[28] Because of the low isoelectric point of AtPCNAs, we were not able to immobilize the PCNA protein on the chip. Thus, we immobilized the same p21 peptide as that used for the crystallographic analysis, and then various concentrations of PCNA proteins were passed over the chip (see Fig. 3). The K_D values for the AtPCNA1 and AtPCNA2 interactions with p21 were calculated by the use of the BIAevaluation software, based on the same simple binding model (A + B = AB) as previously used for the evaluation of the interaction between human PCNA and p21.[32] The obtained K_D values (AtPCNA1 $K_D = 5.8 \times 10^{-7}M$, AtPCNA2 $K_D = 5.9 \times 10^{-7}M$) were comparable to each other, suggesting no difference in affinity to the tested p21 fragment. Our data also suggested that the binding between the plant PCNA and the p21 fragment might be functionally significant, although the strength of the affinity is about 10 times lower than that between the human PCNA and the p21 fragment (K_D 5.8 $\times$ $10^{-8}M$). This different affinity is not surprising, considering the fact that the human p21 protein is not an actual homolog of the natural plant PCNA-interacting protein. The strong interaction observed between p21 and AtPCNAs highlights the biological significance and the possible presence of a functional plant p21 homolog, which has not been reported yet. It should also be considered that the peptide used in our studies was only 22 amino acids (140Gly-Ser160) long, and thus is much shorter than the 39 amino acid peptide (126Gln-Pro164) fused to GST, which was used previously.[32]

Analysis of heterotrimerization

The presence of two *PCNA* genes in *A. thaliana* raises an intriguing question about the functional roles of the proteins encoded by these genes. Our two AtPCNA crystal structures did not display obvious differences that could be directly connected with distinct functions. However, a recent report suggested various functions for AtPCNA proteins related to DNA repair.[33] For instance, it was shown that only AtPCNA2 could functionally interact with *Arabidopsis* DNA polymerase η. In fact, the coexpression of DNA polymerase η and AtPCNA2, but not AtPCNA1, restored normal UV resistance in a yeast *RAD30* mutant.

Thus, we tested the possibility of whether AtPCNA1 and AtPCNA2 could adopt heterotrimeric ring structures, which might also have different biological functions *in vivo*. The conserved subunit interface
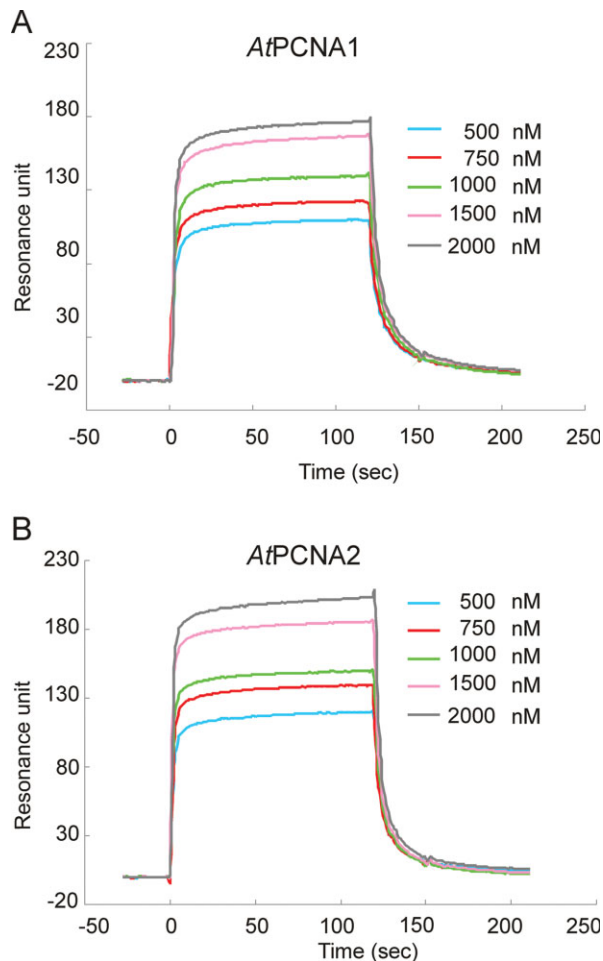
Figure 3. Analyses of interactions between AtPCNA and the C-terminal fragment of human p21. Aliquots (70 μL) of purified AtPCNA proteins at various concentrations (500–2000 nM) were injected at a flow rate of 20 μL/min at 25°C onto chips with the immobilized p21 fragment. The injection was started at time 0 and finished at time 120 s. Sensorgrams for AtPCNA1 and AtPCNA2 are shown on panels **A** and **B**, respectively. The sensorgrams did not show significant differences in binding between the p21 peptide and AtPCNA1 or AtPCNA2.

between the two AtPCNAs [Fig. 1(C)] suggests that these PCNAs may form the heterotrimer in cells.

The AtPCNA1 and AtPCNA2 proteins were coexpressed in *E. coli* and were purified (Materials and Methods, Supporting Information Fig. 3). Gel filtration profiles showed the single peak, which corresponds to the trimer, indicating that coexpressed AtPCNA proteins also form the trimeric ring in solution (data not shown). An analysis of the different migrations of the His-PCNA/PCNA proteins by native gel electrophoresis revealed that the AtPCNA1/2 proteins can form various heterotrimers (Fig. 4, lanes 6 and 8). Indeed, PCNA formed four different PCNA rings (composed of 1/1/1, 1/1/2, 1/2/2, and 2/2/2 monomers) in *E. coli* cells, implying that various heterotrimers with different biological functions could also be expressed in plant cells.

Arabidopsis thaliana PCNA Crystal Structure
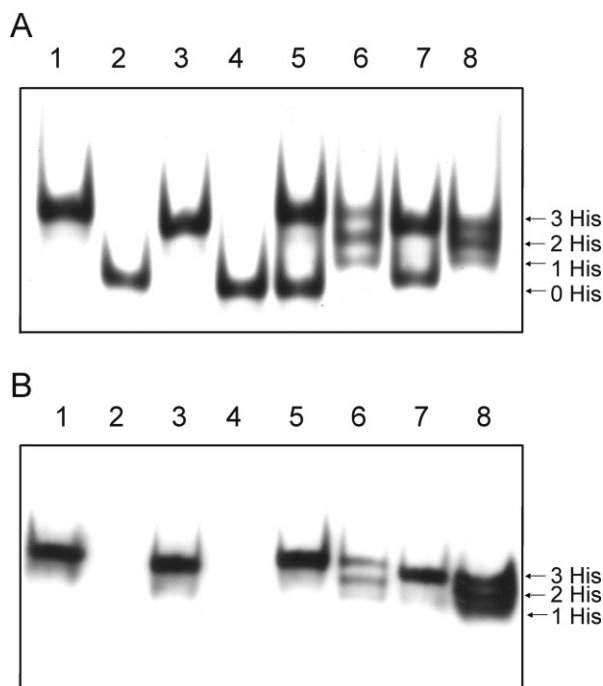
Figure 4. Analysis of heterotrimerization. Purified recombinant proteins were separated by 4% native PAGE in 1× TBE buffer at 4°C. Lane 1: His*At*PCNA1; lane 2: *At*PCNA1; lane 3: His*At*PCNA2; lane 4: *At*PCNA2; lane 5: His*At*PCNA1 and *At*PCNA2 mixed after purification; lane 6: His*At*PCNA1 and *At*PCNA2 overexpressed together in *E. coli* and purified; lane 7: His*At*PCNA2 and *At*PCNA1 mixed after purification; lane 8: His*At*PCNA2 and *At*PCNA1 overexpressed together in *E. coli* and purified. (**A**) Coomassie Brilliant Blue staining. Each protein (5 µg) was separated in the gel. (**B**) Western blotting analysis with the tetra-His horseradish peroxidase antibody conjugate. Each protein (2.5 µg) was separated and subjected to a Western blot analysis.

In contrast to other results that suggested the ring–ring interaction in mammalian cells,[34] we did not observe such an interaction (Fig. 4, lanes 5 and 7). Together with previously published results,[33] our findings suggest that the difference between the *At*PCNA proteins may play important roles in signal transduction pathways. Although the knowledge about plant PCNAs is still limited, we can envisage that different ring compositions might lead to various types of signal transduction in response to specific stimuli. Collectively, these data shed new light on biochemical properties of PCNA in plant cells. In particular, we wonder whether plant PCNA molecules undergo posttranslational modification during DNA damage. In fact, such phenomena are well known in yeast and mammals, in which PCNA is frequently ubiquitinated upon DNA damage.[35]

Materials and Methods

Purification of recombinant His-At*PCNA1* and His-At*PCNA2* proteins

The open reading frames of *At*PCNA1 and *At*PCNA2 were amplified with specific sets of primers: *At*PC-NA1F (5′-GGAATTCCATATGTTGGAGCTACGTCT TGTTC-3′) and *At*PCNA1R (5′-CG GGATCCTTAGGG ATTAGTGTCTTCTTCTTC-3′), and *At*PCNA2F (5′-GGAATTCCATATGttggagcttcgtttag-3′) and *At*PCNA2R (5′-CGGGATCCTTATTCTGGTTTGGTGTCTTC-3′), respectively. The PCR reactions were done in a 50 µL volume, containing 1× PCR buffer (20 mM Tris-HCl, 2 mM MgSO$_4$, 10 mM KCl, 10 mM (NH$_4$)$_2$SO$_4$, 0.1% Triton® X-100 (v/v), BSA 0.1 mg/mL, pH 8.8), 0.2 mM dNTPs, 2.5 U of *Pfu* DNA polymerase (Stratagene), 2 mM of each primer, and 1 ng of template plasmid. The preliminary denaturation was performed at 94°C for 5 min, and 30 cycles of amplification sequentially followed at 94°C for 30 s, 50°C for 30 s, and 72°C for 2 min, and then an incubation at 72°C for 7 min was performed on a thermocycler (Takara). The resulting products were purified, digested with BamHI and NdeI (Takara) restriction enzymes, cloned into the pET15b expression vector using a Ligation High kit (Toyobo), and sequenced. *E. coli* Rosetta cells (Novagen) were transformed using these constructs and grown at 37°C in 2 L LB medium containing ampicillin (100 µg/mL) and chloramphenicol (30 µg/ mL). Isopropyl-β-D-thiogalactopyranoside (IPTG, 1 mM) was then added when the culture reached an OD$_{595}$ of 0.6, and the *At*PCNA proteins were induced at 37°C. After 4 h of induction, the cells were harvested by centrifugation (5000g for 15 min at 4°C), resuspended in 50 mL of buffer A (50 mM NaH$_2$PO$_4$, 300 mM NaCl, and 10 mM imidazole, pH 8.0) containing EDTA-free protease inhibitor cocktail (Roche), and sonicated (10 min, 5 s pulses, 10 s break). All of the following procedures were performed at 4°C. The cells were centrifuged at 35,000g for 30 min, and the cell lysate was loaded onto a 3-mL Ni-NTA agarose column (Qiagen) equilibrated with buffer A. The unbound proteins were removed by a wash with 10 volumes of buffer A containing 20 mM imidazole. The bound proteins were eluted with 10 mL of buffer A containing 250 mM imidazole. Next, using an Amicon 5K filter (Millipore), the proteins were exchanged into buffer B (50 mM Tris, 200 mM NaCl, 0.2 mM EDTA, and 10% glycerol (v/v), pH 8.0), concentrated to 20 mg/mL, and then frozen in liquid nitrogen and stored at −80°C until use.

Purification of the At*PCNA1* and At*PCNA2* proteins

The open reading frames of *At*PCNA1 and *At*PCNA2 were cloned into the pET29a vector, as described earlier for pET15b, using the same sets of primers (materials and methods). *E. coli* Rosetta cells (Novagen) were transformed using these constructs and grown at 37°C in 2 L LB medium containing kanamycin (100 mg/mL) and chloramphenicol (30 µg/mL) until the culture reached an OD$_{595}$ of 0.6. The production of the *At*PCNA proteins was then induced with 1l mM IPTG at 37°C. After 4 h of induction, the cells were

harvested by centrifugation (5000*g* for 15 min at 4°C), resuspended in 50 mL of 50 m*M* Tris, pH 8.0, containing EDTA-free protease inhibitor cocktail (Roche), and sonicated (10 min, 5 s pulses, 10 s break). All of the following procedures were performed at 4°C. The cells were centrifuged at 35,000*g* for 30 min. Ammonium sulfate was added to the supernatant to 40% saturation. The suspension was stirred for 20 min and centrifuged at 35,000*g* for 30 min. The pellet was discarded, and then ammonium sulfate was added to the supernatant again to 60% saturation. This suspension was stirred for 20 min and centrifuged at 35,000*g* for 30 min. The precipitate was dissolved in 50 mL of 50 m*M* Tris, pH 7.6, containing 1*M* ammonium sulfate, and was applied to a 5-mL HiTrap Phenyl FF column (Pharmacia). The unbound proteins were removed by a wash with 10 volumes of the same buffer. The bound proteins were eluted with 25 mL of 50 m*M* Tris, pH 7.6, dialyzed against 50 m*M* Tris, pH 7.6, and applied to a 5-mL HiTrap Q HP column (Pharmacia). The unbound proteins were removed by a wash with 10 volumes of 50 m*M* Tris, pH 7.6, and the proteins were eluted with a 200 mL linear gradient from 0.2 to 0.5*M* NaCl in 50 m*M* Tris, pH 7.6. Fractions containing highly pure *At*PCNA were pooled, exchanged into buffer B with an Amicon 5K filter (Millipore), concentrated to 20 mg/mL, and then frozen in liquid nitrogen and stored at −80°C until use.

Analysis of heterotrimerization

The sets of constructs, pET15b*At*PCNA1 and pET29a *At*PCNA2, and pET15b*At*PCNA2 and pET29a*At*PCNA1, were introduced into *E. coli* Rosetta cells (Novagen). The strains were grown at 37°C in 2 L LB medium containing ampicillin (100 μg/mL), kanamycin (100 μg/mL), and chloramphenicol (30 μg/mL). When the OD_{595} of the culture reached 0.6, the temperature was lowered to 20°C, and then the production of the *At*PCNA proteins was induced with 1 m*M* IPTG overnight. The expressed proteins were purified for His-*At*PCNA1 and His-*At*PCNA2 as described earlier, and thus *At*PCNAs trimeric rings without any His-tags were removed in the step using Ni-NTA agarose column. They were then fractionated by 4% native PAGE and analyzed by Western blotting or Coomassie Brilliant Blue staining.

Western blotting

His*At*PCNA1, *At*PCNA1, His*At*PCNA2, *At*PCNA2, and the heterotrimer were separated by 4% native PAGE in 1× TBE buffer and electrotransferred onto a PVDF membrane (0.2 μm) (Millipore), as described previously.[36] After the transfer, the membrane was blocked with PBS containing 10% (w/v) fat-free milk and 0.1% (v/v) Tween 20 for 1 h. The membrane was incubated with a tetra-His horseradish peroxidase antibody conjugate for 1 h at room temperature (Qiagen, dilution 1:1000). After three washes in PBS supplemented with

0.1% (v/v) Tween 20, immunodetection was performed using the ECL Plus Western blotting detection system (Amersham, Pharmacia) at room temperature.

Crystallization and X-ray analysis

Each peptide complex of *A. thaliana* His-PCNA1 and His-PCNA2 was obtained by mixing a 1.5 molar excess of the synthetic p21 peptide (139GRKRRQTSMT DFYHSKRRLIFS160) with His-*At*PCNA (20 mg/mL). Moreover, in the case of the His-*At*PCNA1-p21 complex, 0.5 m*M* DNA duplex (10/14) was added, as described previously,[37] although it was later found that the crystal contained no DNA. These complexes were crystallized by the hanging drop vapor diffusion method at 293 K. In both cases, diffraction quality crystals were obtained using a reservoir containing 100 m*M* citric acid (pH 4.5) and 1.8*M* ammonium sulfate. The complexes were crystallized in two crystal forms. The form 1 crystals belonged to the space group R32, with unit cell constants: $a = b = 110.10$ Å, $c = 403.93$ Å, and contained two PCNA–peptide complexes per asymmetric unit. The form 2 crystals, belonging to the space group R3, with unit cell constants $a = b = 223.70$ Å, and $c = 200.88$ Å, contained eight complex molecules per asymmetric unit. X-ray diffraction data of the crystals were collected on BL38-B1 at SPring-8 (Harima, Japan). The wavelength was set to 1.0000 Å, and a Jupiter-210 CCD detector (Rigaku/MSC Corporation) was used to record the diffractions images. Data sets were processed by the HKL2000 package.[38] The crystals were soaked in reservoir solution supplemented with 30% (v/v) ethylene glycol before flash cooling. The crystals were kept in a 100 K dry-N_2 stream (Rigaku) during data collection. The data collection statistics are summarized in Supporting Information Table I.

The *A. thaliana* PCNA1-p21 peptide complex structure was determined by molecular replacement, using the program CNS and the human PCNA-p21 peptide complex as a probe. Only the PCNA subunit was used for the structure determination. The two subunits at the correct positions were refined using the programs CNS[39] and O.[40] After the initial crystallographic refinement cycles, the bound p21 peptides were clearly visible in the electron density maps, and atomic models for the peptides were built. The protein–peptide complex structure was further refined to convergence. The structure of the *At*PCNA2–peptide complex was determined by molecular replacement, using the program CNS and the *At*PCNA1 structure as a probe. Crystallographic refinements were reiterated to obtain satisfactory convergence. The crystallographic statistics are summarized in Supporting Information Table I. The atomic coordinates have been deposited in the Protein Data Bank, under the accession codes 2ZVV and 2ZVW, for the *At*PCNA1 and *At*PCNA2 complexes, respectively.

Arabidopsis thaliana PCNA Crystal Structure

Surface plasmon resonance analysis

The experiments were performed using a BIACORE 2000 (Biacore AB, Sweden) in running buffer (10 mM HEPES, 150 mM NaCl, 3 mM EDTA, and 0.005% surfactant (v/v), pH 7.4). The human p21 fragment (2.5 µg in 50 µL) was injected over the sensor chip (Sensor Chip CM5, Biacore AB, Sweden) and linked by carbodiimide-coupling, following the manufacturer's protocol. The purified AtPCNA protein solutions (70 µL) at various concentrations were injected at a flow rate of 20 µL/min at 25°C. The association and dissociation of AtPCNAs and the p21 fragment were indicated as shifts in resonance units during the injection and after the exchange to running buffer. Dissociation and association rate constants (K_{diss} and K_{ass}) were obtained with a simple binding model of A + B = AB, using the BIAevaluation 2.1 software (Biacore AB, Sweden), and K_D values were calculated as the ratios of these values.

References

1. Miyachi K, Fritzler MJ, Tan EM (1978) Autoantibody to a nuclear antigen in proliferating cells. J Immunol 121: 2228–2234.
2. Tan CK, Castillo C, So AG, Downey KM (1986) An auxiliary protein for DNA polymerase δ from fetal calf thymus. J Biol Chem 261:12310–12316.
3. Bravo R, Frank R, Blundell PA, Macdonald-Bravo H (1987) Cyclin/PCNA is the auxiliary protein of DNA polymerase-δ. Nature 326:515–517.
4. Prelich G, Tan CK, Kostura M, Mathews MB, So AG, Downey KM, Stillman B (1987) Functional identity of proliferating cell nuclear antigen and a DNA polymerase-δ auxiliary protein. Nature 326:517–520.
5. Krishna TS, Kong XP, Gary S, Burgers PM, Kuriyan J (1994) Crystal structure of the eukaryotic DNA polymerase processivity factor PCNA. Cell 79:1233–1243.
6. Gulbis JM, Kelman Z, Hurwitz J, O'Donnell M, Kuriyan J (1996) Structure of the C-terminal region of p21(WAF1/CIP1) complexed with human PCNA. Cell 87: 297–306.
7. Matsumiya S, Ishino Y, Morikawa K (2001) Crystal structure of an archaeal DNA sliding clamp: proliferating cell nuclear antigen from *Pyrococcus furiosus*. Protein Sci 10: 17–23.
8. Kong XP, Onrust R, O'Donnell M, Kuriyan J (1992) Three dimensional structure of β subunit of *E. coli* DNA polymerase III holoenzyme: a sliding DNA clamp. Cell 69:425–437.
9. Shamoo Y, Steitz TA (1999) Building a replisome from interacting pieces: sliding clamp complexed to a peptide from DNA polymerase and a polymerase editing complex. Cell 99:155–166.
10. Moldvan GL, Pfander B, Jentsch S (2007) PCNA, the Maestro of the replication fork. Cell 129:665–679.
11. Kelman Z (1997) PCNA: structure, functions and interactions. Oncogene 14:629–640.
12. Bauer GA, Burgers PM (1990) Molecular cloning, structure and expression of the yeast proliferating cell nuclear antigen gene. Nucleic Acids Res 18:261–265.
13. Waseem NH, Labib K, Nurse P, Lane DP (1992) Isolation and analysis of the fission yeast gene encoding polymerase δ accessory protein PCNA. EMBO J 11:5111–5120.
14. Almendral JM, Huebsch D, Blundell PA, Macdonald-Bravo H, Bravo R (1987) Cloning and sequence of the human nuclear protein cyclin: homology with DNA-binding proteins. Proc Natl Acad Sci USA 84:1575–1579.
15. Matsumoto K, Moriuchi T, Koji T, Nakane PK (1987) Molecular cloning of cDNA coding for rat proliferating cell nuclear antigen (PCNA)/cyclin. EMBO J 6:637–642.
16. Yamaguchi M, Hayashi Y, Hirose F, Matsuoka S, Moriuchi T, Shiroishi T, Moriwaki K, Matsukage A (1991) Molecular cloning and structural analysis of mouse gene and pseudogenes for proliferating cell nuclear antigen. Nucleic Acids Res 19:2403–2410.
17. Yamaguchi M, Nishida Y, Moriuchi T, Hirose F, Hui CC, Suzuki Y, Matsukage A (1990) Drosophila proliferating cell nuclear antigen (cyclin) gene: structure, expression during development, and specific binding of homeodomain proteins to its 5′-flanking region. Mol Cell Biol 10: 872–879.
18. Hata S, Kouchi H, Tanaka Y, Minami E, Matsumoto T, Suzuka I, Hashimoto J (1992) Identification of carrot cDNA clones encoding a second putative proliferating cell nuclear antigen, DNA polymerase δ auxiliary protein. Eur J Biochem 203:367–371.
19. Lopez I, Khan S, Vazquez-Ramos J, Hussey PJ (1995) Molecular cloning of a maize cDNA clone encoding a putative proliferating cell nuclear antigen. Biochim Biophys Acta 1260:119–121.
20. Lopez I, Khan S, Vazquez J, Hussey PJ (1997) The proliferating cell nuclear antigen (PCNA) gene family in *Zea mays* is composed of two members that have similar expression programmes. Biochim Biophys Acta 1353:1–6.
21. Suzuka I, Hata S, Matsuoka M, Kosugi S, Hashimoto J (1991) Highly conserved structure of proliferating cell nuclear antigen (DNA polymerase δ auxiliary protein) gene in plants. Eur J Biochem 195:571–575.
22. Strzalka W, Ziemienowicz A (2007) Molecular cloning of *Phaseolus vulgaris* cDNA encoding proliferating cell nuclear antigen. J Plant Physiol 164:209–213.
23. Cann IK, Ishino S, Hayashi I, Komori K, Toh H, Morikawa K, Ishino Y (1999) Functional interactions of a homolog of proliferating cell nuclear antigen with DNA polymerases in Archaea. J Bacteriol 181:6591–6599.
24. Bauer GA, Burgers PM (1988) The yeast analog of mammalian cyclin/proliferating-cell nuclear antigen interacts with mammalian DNA polymerase δ. Proc Natl Acad Sci USA 85:7506–7510.
25. Ng L, Prelich G, Anderson CW, Stillman B, Fisher PA (1990) Drosophila proliferating cell nuclear antigen. Structural and functional homology with its mammalian counterpart. J Biol Chem 265:11948–11954.
26. Matsumoto T, Hata S, Suzuka I, Hashimoto J (1994) Expression of functional proliferating cell nuclear antigen from rice (*Oryza sativa*) in *Escherichia coli*. Activity in association with human DNA polymerase δ. Eur J Biochem 223:179–187.
27. Laquel P, Litvak S, Castroviejo M (1993) Mammalian proliferating cell nuclear antigen stimulates the processivity of two wheat embryo DNA polymerases. Plant Physiol 102:107–114.

28. Ball KL, Lane DP (1996) Human and plant proliferating-cell nuclear antigen have a highly conserved binding site for the p53-inducible gene product p21WAF1. Eur J Biochem 237:854–861.

29. Warbrick E (2000) The puzzle of PCNA's many partners. Bioessays 22:997–1006.

30. Matsumiya S, Ishino S, Ishino Y, Morikawa K (2002) Physical interaction between proliferating cell nuclear cell antigen and replication factor C from *Pyrococcus furiosus*. Genes Cells 7:911–922.

31. Landau M, Mayrose I, Rosenberg Y, Glaser F, Martz E, Pupko T, Ben-Tal N (2005) ConSurf 2005: the projection of evolutionary conservation scores of residues on protein structures. Nucleic Acids Res 33:W299–W302.

32. Oku T, Ikeda S, Sasaki H, Fukuda K, Morioka H, Ohtsuka E, Yoshikawa H, Tsurimoto T (1998) Functional sites of human PCNA which interact with p21 (Cip1/Waf1), DNA polymerase δ and replication factor C. Genes Cells 3:357–369.

33. Anderson JJ, Vonarx EJ, Pastushok L, Nakagawa M, Katafuchi A, Gruz P, Di Rubbo A, Grice DM, Osmond MJ, Sakamoto AN, Nohmi T, Xiao W, Kunz BA (2008) *Arabidopsis thaliana* Y-family DNA polymerase ε catalyses translesion synthesis and interacts functionally with PCNA2. Plant J 55:895–908.

34. Naryzhny SN, Zhao H, Lee H (2005) Proliferating cell nuclear antigen (PCNA) may function as a double homo-trimer complex in the mammalian cell. J Biol Chem 280:13888–13894.

35. Hoege C, Pfander B, Moldovan GL, Pyrowolakis G, Jentsch S (2002) RAD6-dependent DNA repair is linked to modification of PCNA by ubiquitin and SUMO. Nature 419:120–121.

36. Towbin H, Staehelin T, Gordon J (1979) Electrophoretic transfer of proteins from polyacrylamide gels to nitrocellulose sheets: procedure and some applications. Proc Natl Acad Sci USA 76:4350–4354.

37. Georgescu RE, Seung-Sup K, Yurieva O, Kuriyan J, Kong XP, O'Donnell M (2008) Structure of a sliding clamp on DNA. Cell 132:43–54.

38. Otwinowski Z, Minor W (1997) Processing of X-ray diffraction data collected in oscillation mode. Methods Enzymol 276:307–326.

39. Brünger AT, Adams PD, Clore GM, DeLano WL, Gros P, Grosse-Kunstleve RW, Jiang JS, Kuszewski J, Nilges M, Pannu NS, Read RJ, Rice LM, Simonson T, Warren GL (1998) Crystallography and NMR system: a new software suite for macromolecular structure determination. Acta Crystallogr D Biol Crystallogr 54:905–921.

40. Jones TA, Zou JY, Cowan SW, Kjeldgaard M (1991) Improved methods for building protein models in electron density maps and the location of errors in these models. Acta Crystallogr A 47:110–119.